Journal of Plant Physiology 177 (2015) 128–138

Contents lists available at ScienceDirect

Journal of Plant Physiology

journal homepage: www.elsevier.com/locate/jplph

Variations between the photosynthetic properties of elite and landrace Chinese rice cultivars revealed by simultaneous measurements of 820 nm transmission signal and chlorophyll *a* fluorescence induction

Saber Hamdani[a], Mingnan Qu[a], Chang-Peng Xin[a], Ming Li[a], Chengcai Chu[b], Govindjee[c], Xin-Guang Zhu[a,*]

[a] *CAS Key Laboratory of Computational Biology, Partner Institute for Computational Biology, Shanghai Institutes for Biological Sciences, Chinese Academy of Sciences, Shanghai 200031, China*
[b] *Institute of Genetics and Developmental Biology, Chinese Academy of Sciences, Beijing 100101, China*
[c] *Department of Biochemistry, Department of Plant Biology, and Center of Biophysics and Quantitative Biology, University of Illinois at Urbana Champaign, Urbana, IL 61801, USA*

ARTICLE INFO

Article history:
Received 15 September 2014
Received in revised form
21 November 2014
Accepted 8 December 2014
Available online 17 February 2015

Keywords:
Chlorophyll *a* fluorescence transient
Ferredoxin NADP$^+$ reductase
NADP pool
Oryza sativa
820 nm transmission

ABSTRACT

The difference between the photosynthetic properties of elite and landrace Chinese rice cultivars was studied, using chlorophyll *a* fluorescence induction (mostly a monitor of Photosystem II activity) and I_{820} transmission signal (mostly a monitor of Photosystem I activity) to identify potential photosynthetic features differentiating these two groups, which show different degrees of artificial selection and grain yields. A higher fluorescence (related to PSII) IP rise phase and a lower P700$^+$ (related to PSI) accumulation were observed in the elite cultivars as compared to the landraces. Using these data, together with simulation data from a kinetic model of fluorescence induction, we show that the high IP rise phase and the low P700$^+$ accumulation can be a result of transient block on electron transfer and traffic jam on the electron acceptor side of PSI under a high [NADPH]/[NADP$^+$] ratio. Considering that the ferredoxin NADP$^+$ reductase (FNR) transcript levels of XS134 (a representative elite cultivars) remains unaffected during the first few minutes of light/dark transition compared to Q4145 (a representative landrace cultivars), which shows a strong decline during the same time range, we propose that the FNR of elite cultivars may take more time to be inactivated in darkness. During this time the FNR enzyme can continue to reduce NADP$^+$ molecules, leading to initially high [NADPH]/[NADP$^+$] ratio during OJIP transient. These data suggested a potential artificial selection of FNR during the breeding process of these examined elite rice cultivars.

Introduction

Photosynthesis is one of the most powerful and life-giving biological processes occurring on our Earth (Blankenship, 2014). Oxygenic photosynthesis is carried out on a large scale by plants, algae and cyanobacteria, where light energy is converted into stable-rich chemical compounds, with concomitant uptake of CO_2 and release of O_2 (Eaton-Rye et al., 2012). This process, as well as anoxygenic photosynthesis (Hunter et al., 2009) carried out by photosynthetic bacteria, is responsible for all life on Earth. The photosynthetic apparatus of higher plants includes, in addition to the enzymes involved in CO_2 assimilation, four membrane bound protein complexes (Ke, 2001; Wydrzynski et al., 2005; Golbeck, 2006; Shevela et al., 2013): (1) photosystem II (PSII), water-plastoquinone

Abbreviations: Chl, chlorophyll; DBMIB, 2,5-dibromo-3-methyl-6-isopropyl-*p*-benzo-quinone; DCMU, 3,4-dichlorophenyl-1,1-dimethylurea; F_o, basal (initial, minimal) level of chlorophyll *a* fluorescence; F_m, maximal level of chlorophyll *a* fluorescence; FNR, ferredoxin NADP$^+$ reductase; F_v, variable chlorophyll *a* fluorescence (=F_m minus F_o); I_{820} nm, transmission signal at 820 nm; LED, light emitting diode; OJIP transient, chlorophyll *a* fluorescence induction where O is for F_o, P is for peak (equivalent to F_m in saturating light) and J and I are inflections between O and P; PC, plastcyanin; PQ, plastoquinone; PQH_2, plastoquinol; PS, photosystem; qRT-PCR, real-time quantitative reverse transcription polymerase chain reaction; RC, reaction centre.

* Corresponding author. Tel.: +86 21 5492 0490; fax: +86 21 5492 0451.
E-mail addresses: zhuxinguang@picb.ac.cn, xinguang.zhu@gmail.com (X.-G. Zhu).

http://dx.doi.org/10.1016/j.jplph.2014.12.019
0176-1617/

oxido-reductase, which catalyzes light driven oxidation of water and reduction of plastoquinone (PQ); (2) photosystem I (PSI), plastocyanin- ferredoxin oxido-reductase, which catalyzes the final stage of light reactions, i.e., reduction of ferredoxin and oxidation of plastcyanin (PC); ferredoxin is reduced via ferredoxin $NADP^+$ reductase (FNR), and by NADPH, formed from $NADP^+$, which, in turn, is reduced by PSI; (3) Cytochrome (cyt) b_6f, which catalyzes the transfer of electrons from plastoquinol (PQH_2) to PC.; and (4) ATP Synthase that uses proton motive force (pmf), which is made up of proton gradient ΔpH and $\Delta\psi$, to produce ATP from ADP and inorganic phosphate. Photochemical events of photosynthesis are initiated by the capture of incident photons by pigments in antenna complexes. Then, absorbed energy is efficiently transferred to photochemical reaction centres (RC), leading, ultimately, to the transfer of electrons through an electron transport chain from water to $NADP^+$, and the production of pmf.

Improvement of photosynthetic capacity of food crops has been considered to be a real challenge for plant scientists and crop breeders (Long et al., 2006; Murchie et al., 2008; Zhu et al., 2008; Evans, 2013), in order to cope with the enormous demand for food in the world. Several biotechnological approaches have been applied, using many targets affecting photosynthetic activity (Reynolds et al., 2000; Leegood, 2002; Long et al., 2006; Feng et al., 2007; Zhu et al., 2010; Ort et al., 2011; Gowik and Westhoff, 2011; Raines, 2011; Parry et al., 2013). Many current efforts to identify options to increase photosynthesis follow a rationale design approach, i.e., first identifying potential targets to engineer the plant, based on the current knowledge of photosynthesis, and then applying targeted engineering of these options, and finally examination of their consequences. Besides this approach, mining natural variations of photosynthesis is also regarded as a promising approach to identify a new genes or alleles for crop improvement. Mining variations can also be used to identify potential factors under natural or artificial selection. Here, we report a case study of variations and correlations of some photosynthetic parameters in two different groups of Chinese rice (*Oryza sativa*) cultivars, which show different degrees of artificial selection and also grain yield. The first group represents the elite cultivars, which exhibits high crop yield (Bao et al., 2006; Deng et al., 2007; Zhou and Yao, 2012), which has been under a strong artificial selection by plant breeders for high performance and is commercially used in China (For further details, see e.g., http://www.ricedata.cn/variety/.) Moreover, several cultivars of elite rice, such as: 9311, Minghui 63 (MH63) and Zhonghua 11 (ZH11) have been used as recurrent parent to produce super hybrid rice (Jiang et al., 2004; Zhang et al., 2012). On the other hand, the second group represents traditional Chinese rice varieties, developed between 1928 and 1996 (called here landraces), which mostly shows low crop yields, and is relatively less used these days.

In this study, Chl *a* fluorescence induction (OJIP, where O is for minimum fluorescence, P is for peak, and J and I are inflections), which reflects a progressive reduction of the PQ pool located on the acceptor side of PSII, and transmission changes at 820 nm (I_{820}), representing the redox level of the RC of PSI, were used to characterize these two groups. The OJIP fluorescence induction curve has been used extensively in photosynthesis physiology research (Govindjee, 1995), mainly due to the ease of measuring the OJIP signal. However, OJIP signal is influenced by a large number of biophysical processes. Hence, it has remained a major challenge to fully interpret the physical mechanism underlying each of individual phases of the OJIP curve, even though a number of theoretical studies are available that have explored this issue (Zhu et al., 2005; Lazar, 2009; Xin et al., 2013). In this study, we first explored the relationship between these parameters between landraces and elite cultivars of rice, and showed that there is a distinct increase in the IP phase in the OJIP curve of the chosen elite cultivars. Then, with a kinetic model of fluorescence induction, we evaluated the potential mechanisms underlying simultaneous changes in the IP phase rise and $P700^+$ accumulation and propose that variations in FNR can be a potential mechanism underlying these changes. Finally, we provided evidence showing that the expression level of *FNR* differed between elite and landraces, suggesting that *FNR* might be a gene under artificial selection during the breeding process.

Materials and methods

Plant material

For our measurements, two groups of Chinese rice (*Oryza sativa*) were used. The first group (elite group) was composed of ten accessions, namely, HE2219, KY131, WCC2, MH63, XS134, DHX-Z, DHX-W, ZH11, WY-4 and 9311. The second group (landraces) was also composed of ten accessions, namely, Ao Chiu 2 Hao (A4010), Chun 118-33 (E4050), Kin Shan Zim (H4080), Pan Ju (J4088), Shui Ya Jien (M4112), 4484 (Q4144), 4595 (Q4145), You-I B (Q4146), Chunjiangzao No. 1 (Q4147), and Wong Chim (X4203). (For further details, see e.g., http://www.ricedata.cn/variety/.)

Growth conditions

Rice seeds from the elite and landrace groups were grown for ~30 days in a soil seed bed located in Beijing (China) (39°55′N, 116°25′E). Then, from early June 2013, seedlings were transplanted into plastic pots (12 L volume) containing commercial peat soil (Pindstrup Substrate no. 4), and then grown under outdoor conditions. Measurements were started from early July 2013. During this period, the average lower temperature range was ~24–26 °C, and the average higher temperature range was ~30–31 °C, whereas the humidity range was ~61–75%.

Chlorophyll (Chl) a fluorescence induction (OJIP) and transmission changes at 820 nm (I_{820})

For a background on the use of Chl *a* fluorescence, see chapters in Papagergiou and Govindjee (2004), and for a basic background on detailed experimental technique, see Kalaji et al. (2014). OJIP and I_{820} measurements were recorded simultaneously using the Multifunctional Plant Efficiency Analyzer (M-PEA) (Hansatech, King Lynn, Norfolk, UK). In this instrument, wavelengths of light (from Light Emitting Diodes, LEDs) are: 625 ± 10 nm for the actinic light; 820 ± 25 nm for the modulated light; and 735 ± 15 nm for the far-red light. Plants were kept overnight at 24 °C in darkness. Then, after a 10-min dark adaptation, the attached uppermost fully expanded leaves were exposed for 0.5 s to saturating orange–red (625 nm) actinic light (5000 μmol photons m^{-2} s^{-1}) and modulated light (820 nm) provided by the LED. Measurements were repeated three to four times for each accession. The ratio of variable fluorescence F_v (the difference between the maximal fluorescence, F_m, fluorescence at the P level, and F_0, fluorescence at the O level) to F_m, i.e., F_v/F_m, was used to evaluate the maximum quantum yield of PSII. For the measurements shown later in Fig. 7, plants were kept overnight at 24 °C in darkness. Then, the attached leaves were light-adapted for 10 min in white light (600 μmol photons m^{-2} s^{-1}) provided by an external lamp projector. After that, Chl *a* fluorescence induction was recorded, as described above, first without, and then after 1, 3, 7, and 10 min dark-adaptation.

RNA isolation and real-time RT-PCR analysis

Total RNA was extracted from mature rice leaves at different dark-time point (0, 1, 3, and 10 min) using Purelink RNA Mini Kit (Invitrogen, Carlsbad, CA) according to manufacturer's instructions. Concentration of each RNA sample was measured

using NanoDrop 2000 spectrophotometer (NanoDrop Technologies). RNA samples were reverse transcribed into cDNA using SuperScript® III Reverse Transcriptase (Invitrogen, USA) according to manufacturer's instructions. The real-time RT-PCR was carried out with LightCycle480 System (Roche Applied Science, Indianapolis, USA). The primers for the *FNR* gene (Os06g0107700) and *actine1* (KC140126.1) were designed using the IDT's website (integrated DNA technologies, USA). The primer sequences were as follows:

FNR Forward: 5′-GAGAACTTCCGGGTCGATTATG-3′ and Reverse: 5′-CACAGCTCTTCCTTGTACTCTG-3′.

*Actine*1 Forward: 5′-CCTGACGGAGCGTGGTTAC-3′ and Reverse: 5′-CCAGGGCGATGTAGGAAAGC-3′.

PCR reactions were performed in 96-well white plates with a volume of 20 μl containing 1 μl of cDNA template (~100 ng), 0.25 μM for each primer, and 2 μl of 10× SYBR Green I PCR Master Mix (Roche Applied Science, Indianapolis, USA). The reactions were subjected to a heating step at 95 °C for 5 min, followed by 40 cycles of denaturation at 95 °C for 10 s, annealing at 58 °C for 20 s and elongation at 72 °C for 20 s. Transcript levels were normalized to that of actin1 (internal control gene). Each PCR reaction was performed in triplicate and the calculated error bars represent the standard deviation from three to four PCR results. Statistical analyses involved the $2^{-\Delta\Delta}$CT method (Livak and Schmittgen, 2001).

The model

We extended an earlier Chl *a* fluorescence induction kinetic model that was developed in 2013 (Xin et al., 2013) to incorporate the P700 (reaction centre of PSI) as well as the NADP(H) pool (Fig. S1). Electron transfer from the PQH_2 pool through PC to P700 was simplified in this model to be just one reaction. Electron transfer from P700 to $NADP^+$ was also simplified to be also one reaction. Reduction of $NADP^+$ is catalyzed by FNR, which depends on the substrate concentration. Thus we have assumed that the electron transfer rate from P700 to $NADP^+$ depends on the $NADP^+$ concentration. The rate of this reaction was calculated as follows:

$$V = K\frac{[NADP^+]}{[NADP^+] + [NADPH]'},$$

where K is the rate constant for electron transfer from P700 to $NADP^+$, $[NADP^+]$ is $NADP^+$ concentration, and [NADPH] is NADPH concentration. The rate constant of electron transfer from P700 to $NADP^+$ was estimated at 500 s^{-1} (see e.g., a review by Govindjee and Björn, 2012). All parameters used in this current model are listed in the paper of Xin et al. (2013) (For further details see Fig. S1 and Table S1).

Data analysis

For quantitative analysis, OJIP traces (Stirbet and Govindjee, 2011, 2012) were fitted with the sum of three first-order kinetics by nonlinear regression using sigma plot (SSI, Richmond, CA, USA):

$$F(t) = F_0 + A_{O-J}(1 - e^{-K_{O-J}t}) + A_{J-I}(1 - e^{-K_{J-I}t}) + A_{I-P}(1 - e^{-K_{I-P}t}),$$

where $F(t)$ is fluorescence at time t, F_0 is initial minimum fluorescence, A_{O-J}, A_{J-I} and A_{I-P} are the amplitudes, and K_{O-J}, K_{J-I} and K_{I-P} are the rate constants of the OJ, JI and IP steps of the fluorescence transient.

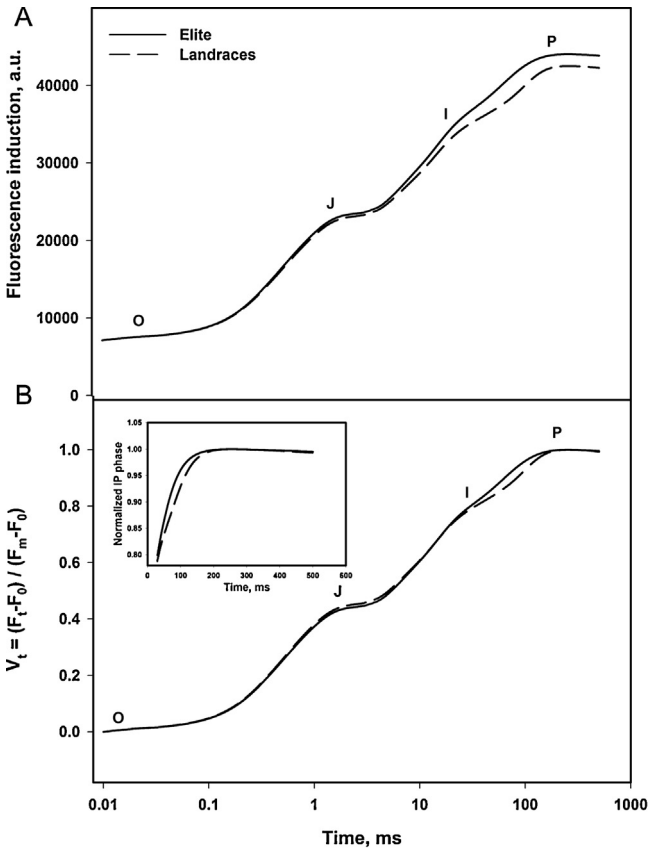

Fig. 1. (A) Chlorophyll (Chl) *a* fluorescence induction curves, measured on rice leaves of elite and landrace groups, are shown on a log time scale. Leaves were dark-adapted for 10 min, and then excited with orange–red (625 nm) actinic light (5000 μmol photons m^{-2} s^{-1}) for 0.5 s. A solid line is for the elite group (average of ten accessions with three to four replications for each accession), and a dashed line is for the landrace group (average of ten accessions with three to four replications for each accession). (B) The OJIP transient was doubly normalized between F_0 (at the O level) and F_M (at the P level), and the data is shown as relative variable fluorescence $V(t) = (F_t - F_0)/(F_M - F_0)$ on a log time scale. (Inset) The IP phase was normalized at the P level.

Results

Chlorophyll (Chl) a fluorescence induction (the OJIP curve)

To analyze photosynthetic activity in both elite and landrace groups, we measured Chl *a* fluorescence induction (OJIP) and plotted it on a log time scale. Fluorescence intensity measures the concentration of reduced Q_A [Q_A^-], which reflects a progressive reduction of the PQ pool located on the acceptor side of PSII. Three main phases are observed: OJ, JI, and IP (Pospisil and Dau, 2000; Zhu et al., 2005; Boisvert et al., 2006; Stirbet and Govindjee, 2011, 2012). The OJIP trace in landrace group shows a typical shape of Chl *a* fluorescence induction curve, as is observed in higher plants at room temperature, with clearly distinguishing phases, as mentioned above. However, the I step in high yielding elite cultivars, as compared to the landraces, is hardly discernible, but the P level is higher (Fig. 1A and Fig. S2). This behavior of the IP phase is similar to that observed in samples treated with DBMIB (2,5-dibromo-3-methyl-6-isopropyl-*p*-benzoquinone), which prevents reoxidation of PQH_2 by cyt b_6f (Bukhov et al., 2003; Schansker et al., 2005; Lazar, 2009). However, the maximum fluorescence (F_m) at the P level remains constant upon DBMIB treatment, contrary to our result here which shows a higher P level in the elite cultivars (Fig. 1A). Fig. 1B shows the same curves as in Fig. 1A, but normalized at both O and P levels. A more quantitative

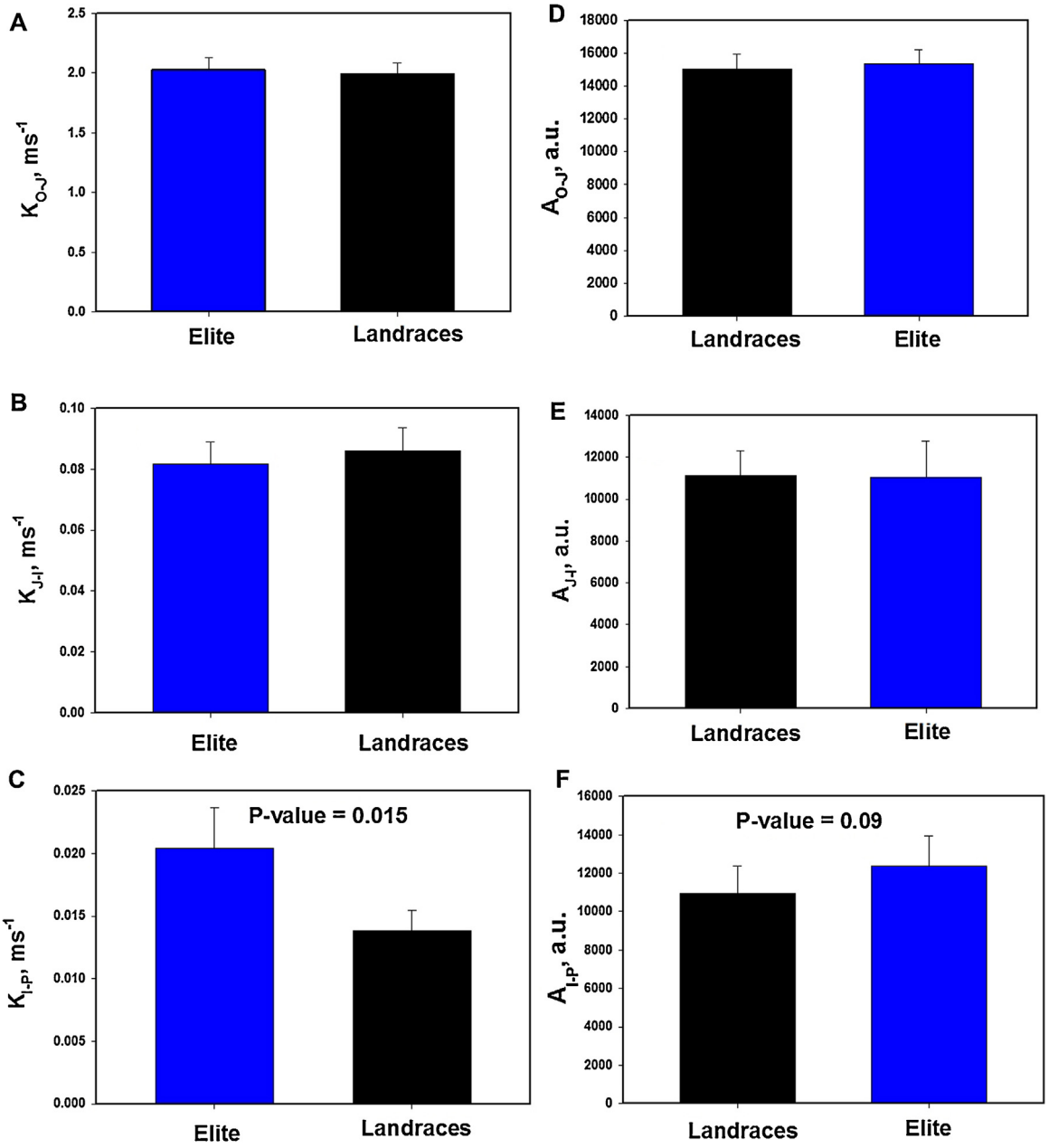

Fig. 2. Rate constant (K) and amplitude (A) of OJ, JI and IP Chl *a* fluorescence rise phases of elite and landrace groups ((A)–(F)). Each group represents the average ± SD of ten accessions with three to four replications for each accession. P values from a t test of the elite and landrace groups are indicated in the graphs. All parameters were deduced from the OJIP fluorescence traces. See Materials and methods for further details.

view is presented in the inset of Fig. 1B that shows a comparison of the variation of the kinetics of IP phase between the elite and landrace groups.

In order to quantitatively estimate the contribution of each step of OJIP trace, we simulated this trace by the sum of three exponential components that represent the OJ, JI and IP phases. Three parameters were deduced from this simulation, i.e., the rate constant (K), the amplitude (A), and the half-time ($t^{1/2}$) of these three steps. Among the parameters measured, only K_{I-P} and $t^{1/2}{}_{I-P}$ show a significant difference between elite and landrace groups, $t^{1/2}{}_{I-P}$ being ~25% smaller, and K_{I-P} being ~54% larger in the elite group, as compared to the landraces (Fig. 2 and Table 1). However, the A_{I-P} is slightly increased in the elite cultivars. As mentioned above, the K_{I-P} is higher in the elite cultivars compared to the landraces (0.02 ± 0.0032 versus $0.013 \pm 0.0016\,ms^{-1}$), meaning that the elite group is able to reach the F_m faster than the other group. However, no significant variation in the maximum quantum yield of PSII, as evaluated from F_v/F_m, is observed (Table 1 and Table S2). This result suggests a subtle but significant modification in the electron transfer process in the elite group.

Table 1
Quantitative analysis of OJIP traces in both elite and landrace groups. Half-times ($t^{1/2}$) corresponding to OJ, JI and IP phases were deduced from the equation: $F(t) = F_0 + A_{O-J}(1 - e^{-KO-J\,t}) + A_{J-I}(1 - e^{-KJ-I\,t}) + A_{I-P}(1 - e^{-KI-P\,t})$. Also shown are F_v/F_m values. Results are averages ± SD (n = 30–40).

	$t^{1/2}{}_{O-J}$ (ms)	$t^{1/2}{}_{J-I}$ (ms)	$t^{1/2}{}_{I-P}$ (ms)*	F_v/F_m
Elite	0.34 ± 0.019	8.69 ± 0.7	39.4 ± 7.6	0.84 ± 0.005
Landraces	0.35 ± 0.016	8.14 ± 0.7	52.8 ± 6.6	0.83 ± 0.006

* P-value = 0.015.

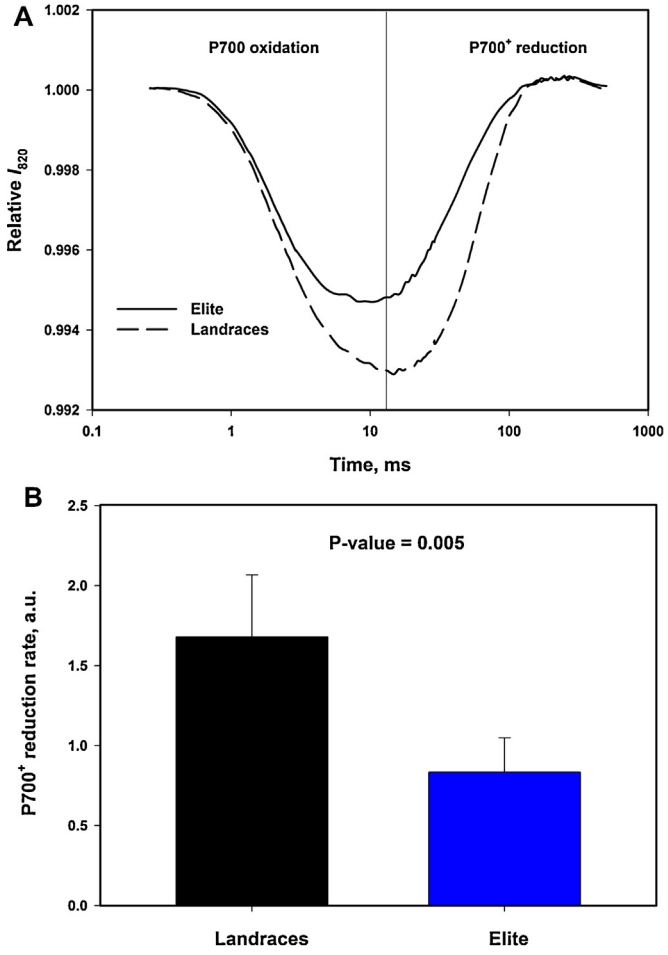

Fig. 3. (A) Transmission changes at 820 nm (I_{820}) measured after a 0.5-s pulse of orange–red (625 nm) actinic light (5000 μmol photons m^{-2} s^{-1}) in rice leaves. A solid line is for the elite group (average of ten accessions with three to four replications for each accession), and a dashed line is for the landrace group (average of ten accessions with three to four replications for each accession). The vertical solid line indicates the possible start and end of the P700 oxidation and the $P700^+$ reduction phases, respectively. (B) $P700^+$ reduction rate calculated from the slope of the $P700^+$ reduction phase, shown in (A), the upper panel. Data in each group are the average ± SD of ten accessions with three to four replicates for each accession. A *P* value from a *t* test of the elite and landrace groups was 0.005.

Transmission changes at 820 nm (I_{820})

To gain further information about the electron transfer process at the two ends of the electron transport chain, I_{820}, which mainly measures oxidation and reduction of RC of PSI, P700, was recorded simultaneously with Chl *a* fluorescence induction. Fig. 3 shows transmission change kinetics at 820 nm during 0.5 s of orange–red (625 nm) actinic light illumination (5000 μmol photons m^{-2} s^{-1}). Changes in I_{820} reflect modification not only in the redox state of the RC of PSI, P700, as mentioned above, but also of PC. Oxidation of P700 and PC is known to cause a decrease in transmission (or increase in absorption) in the 800–850 nm range (Harbinson and Woodward, 1987; Harbinson and Hedley, 1989; Klughammer and Schreiber, 1994). On the other hand, reversal of the transmission decrease is mainly induced by the arrival of electrons from PSII (Schansker et al., 2003). In our experimental data, two major features are observed in the kinetics of transmission change at 820 nm between elite and landrace groups. We have observed a lesser accumulation of $P700^+$ and a slower reduction rate in elite cultivars compared to landraces (Fig. 3A and Fig. S3). A quantitative view is presented in Fig. 3B, which shows that the $P700^+$ reduction rate of elite cultivars is almost half of that recorded in landraces.

Correlations

According to our experimental data, photosynthetic parameters are significantly different in elite cultivars as compared to those in landraces. These differences can be summarized with two major points: (1) higher and faster IP phase; and (2) lower $P700^+$ reduction rate, observed in elite as compared to landraces (Figs. 1–3). In order to further investigate the relationship between these parameters, a series of correlation analysis was done (Fig. 4). A relatively high negative correlation is observed between the $P700^+$ reduction rate and K_{I-P} (Fig. 4A), meaning that the higher and faster IP phase is closely related to the lower $P700^+$ reduction rate observed in elite group. Finally, a moderate negative correlation between F_v/F_m and $P700^+$ reduction rate is observed (Fig. 4B). However, F_v/F_m and K_{I-P} are strongly correlated with each other (Fig. 4C).

Simulations

To gain deeper insight into the mechanisms underlying the variations in the elite cultivars in the parameters related to the photosynthetic light reactions, we used an updated version of a model of Chl *a* fluorescence induction kinetics (Xin et al., 2013). Fig. 5A shows our results on parallel measurement on the OJIP transient and the I_{820} with the M-PEA instrument on both the elite and landrace groups. To simulate our experimental data, we considered two possible scenarios: (1) high [NADPH]/[$NADP^+$] ratio; and (2) a small NADP pool size. The simulated OJIP curve of the control shows J, I and P steps at positions that are very close to the experimental data. However, the I_{820} curve is shifted to shorter times (Fig. 5B and C). Further, a good qualitative agreement is found when the theoretical OJIP curves, in both high [NADPH] and small NADP pool size conditions, are compared with our experimental data (Fig. 5B and C). Such behavior suggests that the IP rise recorded in the elite cultivars can be related to limitation on the acceptor side of PSI (a "traffic jam" Munday and Govindjee, 1969), leading to a transient block in electron transfer on the electron acceptor side of PSII. However, less convincing simulation is found when the theoretical I_{820} curves are compared with related experimental data. In fact, the significant variation in the minimum of I_{820} (reflecting the maximum $P700^+$ accumulation) and the rate of $P700^+$ reduction, measured in experimental data, are missing in the simulation data, especially for the small NADP pool size condition (Fig. 5C). This poor fit can be understood by the difficulties encountered in carefully simulating the I_{820} signal, which needs further studies on the factors that control this signal.

As seen in our simulation data, the best fit is found under high [NADPH] conditions (Fig. 5B). This situation suggests that all the electron acceptors of PSI must be reduced, which in turn causes a transient block in electron transfer through the two photosystems, as already mentioned above. To gain further insight on the redox changes in all the PQ components (Q_A; Q_B; and PQ), we predict, as implied above, that the relative concentration of [Q_A^-], [Q_B^{2-}], [$Q_A^- Q_B^{2-}$] and [PQH_2] must be high under high [NADPH] conditions (Fig. 6). The main point deduced from this simulation data is that all PQ components are in much more reduced state during the IP phase, compared to the controls (Fig. 6A–D). This increase of redox components is proportional to the increase of IP phase of elite cultivars. Such a result supports our hypothesis, which envisions a transient block in the electron transfer process under high [NADPH] conditions. This blockage can be explained by an increase of the reduced state of all PQ components during the IP phase (Stirbet and Govindjee, 2011, 2012).

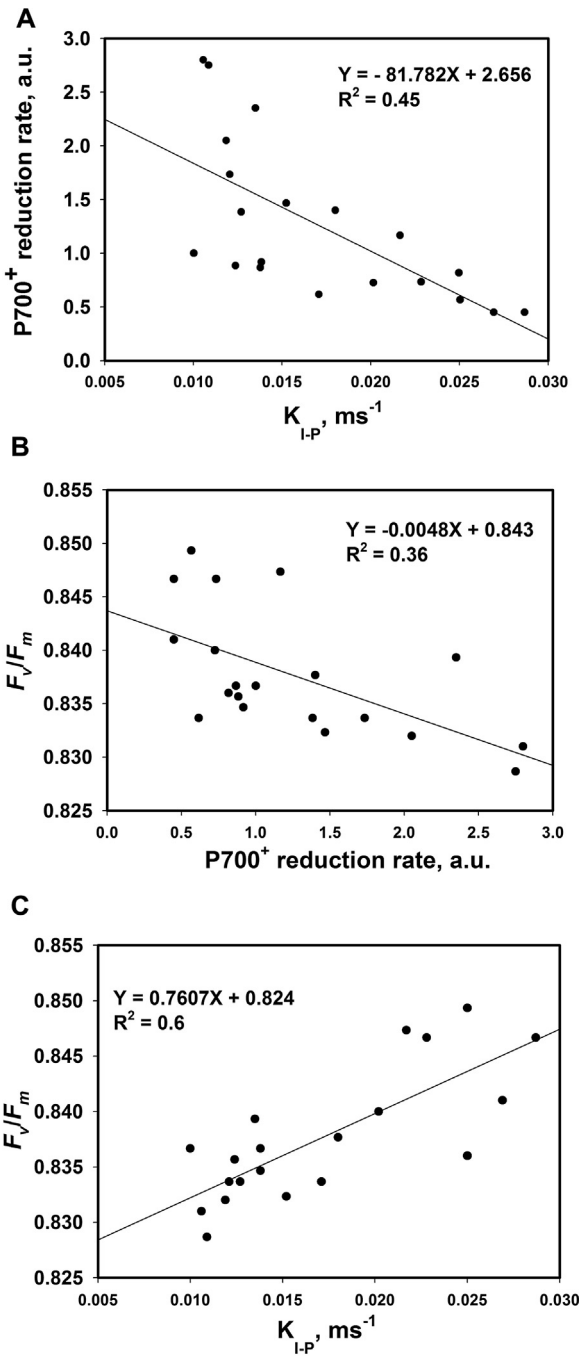

Fig. 4. Relationship between photosynthetic parameters deduced from Chl *a* fluorescence induction and transmission changes at 820 nm. (A) Negative correlation between $P700^+$ reduction rate and K_{I-P}. (B) Negative correlation between F_v/F_m and $P700^+$ reduction rate. (C) Positive correlation between F_v/F_m and K_{I-P}. Each point represents the average of three to four replicates. The regression lines represent all twenty accessions (10 elite + 10 landraces). The regression coefficients (R^2) and equations are shown in individual panels.

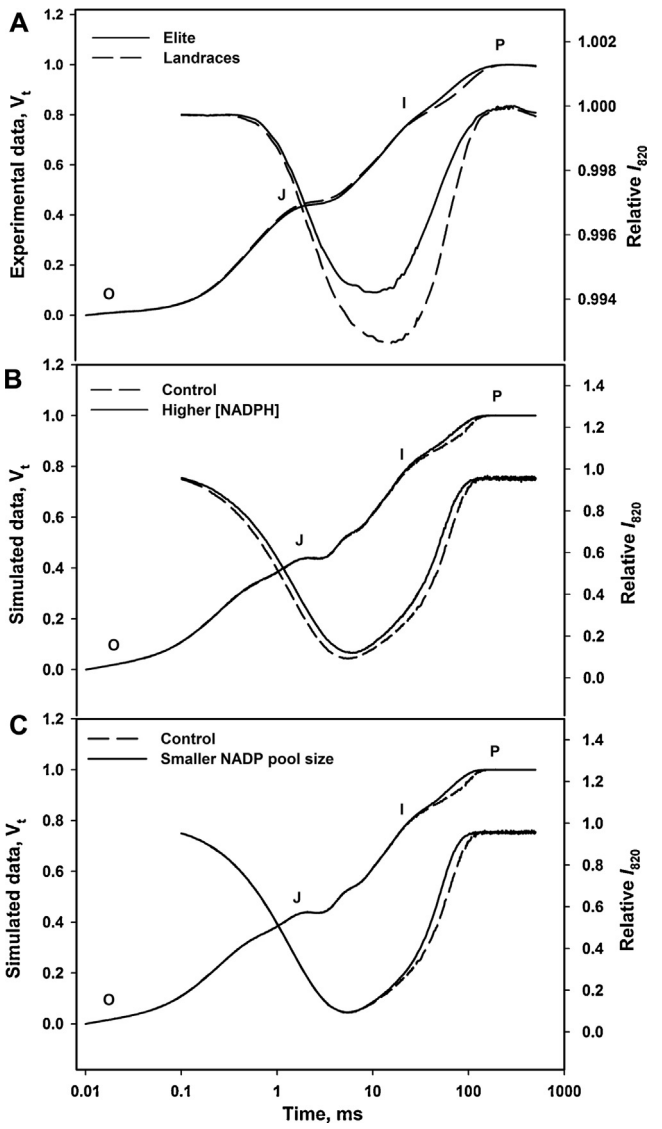

Fig. 5. Comparison of the simulated OJIP fluorescence and I_{820} transmission curves with the experimental data (A) under high NADPH concentration (B) or small NADP pool size conditions (C). Results shown in Figs. 2B and 4A were plotted together on the same time scale and presented in the panel A. A solid lines show the elite group (average of ten accessions with three to four replications for each accession), high [NADPH], and small NADP pool size, respectively. Dashed lines show the landrace group (average of ten accessions with three to four replications for each accession), and the control, respectively.

Correlation between FNR dark inactivation and IP phase

To explain the possible cause for the increase in [NADPH]/[$NADP^+$] ratio, suggested for the elite group, we estimated the FNR activity during light/dark transitions. For this purpose, we randomly selected one cultivar from each group (XS134: represents the elite group and Q4145: represents the landrace group). Then, we measured the dark recovery of the IP phase, which correlates with the FNR inactivation in darkness (Schansker et al., 2006). Fig. 7 shows the dark recovery kinetics of the IP phase following a 10-min of light-adaptation. During the first 3 min, about 30% of the IP phase recovery is observed in XS134 cultivar, and the maximum is reached after 10 min of dark. This indicates that the inactivation of FNR in this cultivar is probably around 30% after 3 min and it takes 10 min for it to become completely inactivated (Fig. 7A). However, about 80% of the FNR inactivation is observed after only 3 min dark in Q4145 cultivar (Fig. 7B). This result suggests that the turnover rate of FNR in darkness is different between these two cultivars. For the XS134 cultivar, the FNR enzyme remains activated during the first few minutes of light/dark transitions. However, a strong decline of the FNR activity during the same time range is observed in the Q4145 cultivar.

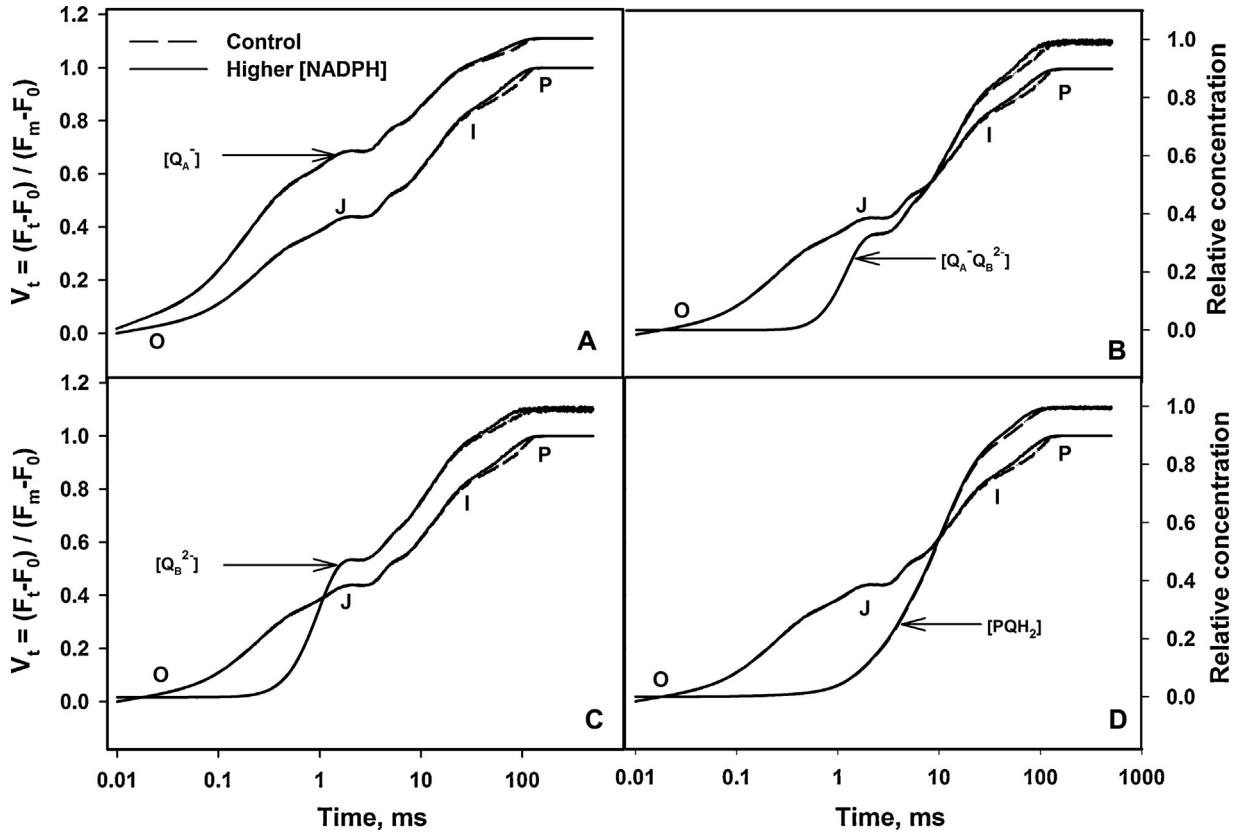

Fig. 6. The predicted influence of a higher [NADPH] conditions on the concentrations of reduced Q_A, reduced Q_B and the PQ pool: (A) $[Q_A^-]$, (B) $[Q_A^-Q_B^{2-}]$, (C) $[Q_B^{2-}]$, and (D) $[PQH_2]$. Simulated OJIP curves and the curves for concentrations of various PQ components were plotted together on the same time scale. Solid lines represent the high [NADPH] conditions, while the dashed lines represent the control.

Real-time RT-PCR

In order to estimate the FNR activity of XS134 and Q4145 cultivars in darkness, we measured changes in transcript levels of the *FNR* gene (Os06g0107700) using the real-time RT-PCR method. Fig. 8 shows variations of the relative mRNA levels between these two cultivars at different dark-time point. During the first 3 min, the mRNA accumulation of *FNR* of XS134 cultivar remains almost unaffected by transition from light to dark, but shows around twofold decrease after 10 min dark. However, around twofold down-regulation of the relative expression level is observed in Q4145 cultivar after 3 min dark, and around 1.5 fold after 10 min dark (Fig. 8A). Moreover, the relative expression level of *FNR* gene is almost 1.5- to 2.5 fold higher in XS134 compared to Q4145 at 1 and 3 min dark, respectively. However, it decreases slightly after 10 min dark (Fig. 8B). This result illustrates clearly a correlation between the dark recovery of the IP phase and the *FNR* expression level. In fact, during the first 3 min of light/dark transitions, a low IP phase and high *FNR* expression level are observed in XS134 cultivar (Figs. 7A and 8A), suggesting that the FNR enzyme remains activated during this time. In contrast, the Q4145 cultivar shows a high IP phase in parallel with low *FNR* expression level during the same time range (Figs. 7B and 8A).

Discussion

In this paper we have explored variations of Chl *a* fluorescence related parameters and transmission changes at 820 nm (I_{820}) in Chinese elite and landraces rice cultivars. Higher IP phase, during Chl *a* fluorescence transient, was accompanied by an increase in the minimum of I_{820} signal (representing P700 oxidation) as recorded in elite cultivars compared to landraces (Fig. 5A). Here, we will first discuss the variations, observed in the OJIP curves, as well as in the I_{820} signal. Then, we will discuss the possible role of changes in FNR in determining these variations. On the basis of these discussions, we have proposed in this paper that FNR might have been under artificial selection during rice breeding process.

Variations of the OJIP curves and the I_{820} signal in elite and landraces cultivars

For an understanding of the parallel measurements of the OJIP curves and the I_{820} signal, see Schansker et al. (2003), Strasser et al. (2010) and Oukarroum et al. (2013). Several theories and hypotheses have attempted to explain the origin of the variable Chl *a* fluorescence during the OJIP transient, measured under continuous saturating light in dark adapted sample (Govindjee, 1995; Lazar, 1999; Samson et al., 1999). It is generally accepted that the OJ rise represents the photochemical phase, and depends mainly on photo-reduction of Q_A in the active PSII centres (Stirbet and Govindjee, 2011, 2012). However, the processes involved during the thermal phase (i.e., J-I-P) are highly controversial, especially for the origin of the IP rise. Several explanations have been given to explain the process underlying the IP phase (Munday and Govindjee, 1969; Schreiber and Vidaver, 1976; Vernotte et al., 1979; Satoh, 1981; Hsu and Leu, 2003). It was thought that the IP phase occurs when the oxidized PQ pool, which acts as a quencher of fluorescence, is reduced and, thus, the fluorescence rises (Samson and Bruce, 1996; Prasil et al., 1996). Moreover, Schreiber and Vidaver (1976) have suggested that energy redistribution between PSII and PSI maybe the reason for the IP phase; this implies that the

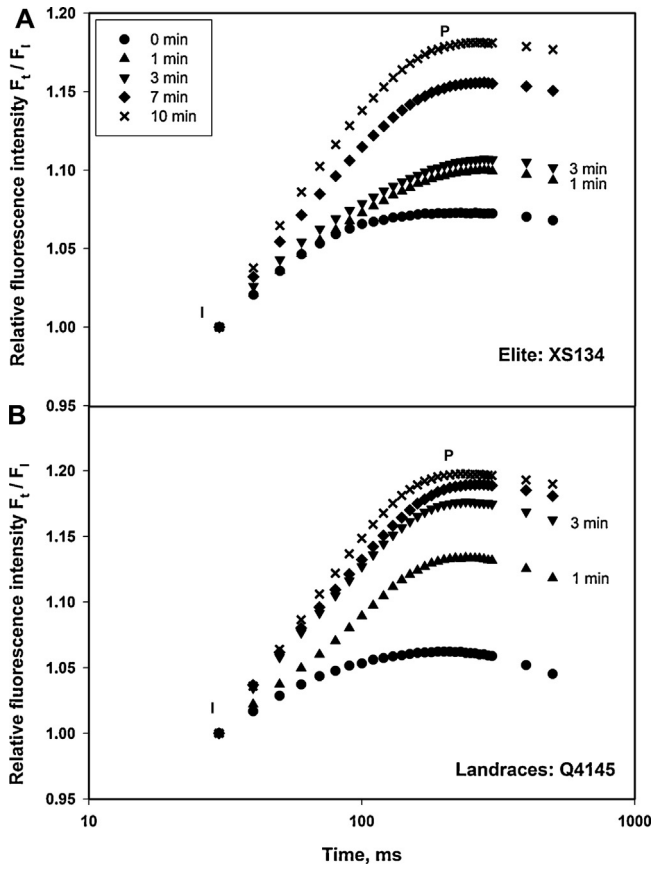

Fig. 7. Dark recovery of the IP phase of Chl *a* fluorescence, measured on rice leaves of XS134, an elite cultivar (A) and Q4145, a landrace cultivar (B) is shown on a log time scale. Attached leaves were light-adapted for 10 min to white light (600 μmol photons m^{-2} s^{-1}), and then excited with orange–red (625 nm) actinic light (5000 μmol photons m^{-2} s^{-1}) for 0.5 s at different dark-times (0, 1, 3, 7 and 10 min). The IP curves were normalized to F_I (fluorescence at I level) and each curve represents the average of three replications.

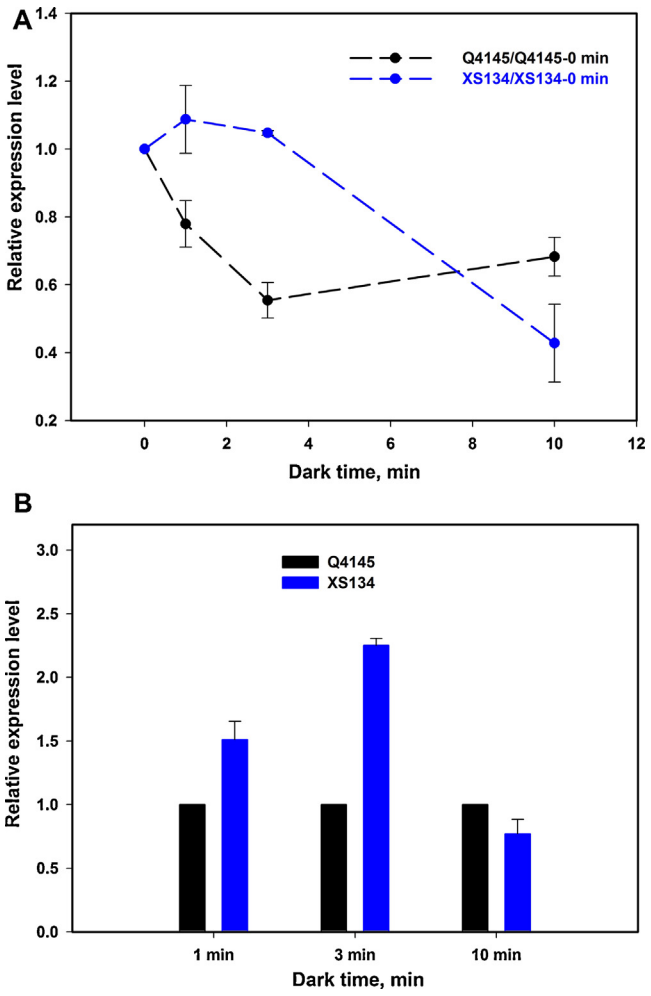

Fig. 8. Transcript levels of *FNR* gene (Os06g0107700) of XS134 and Q4145 cultivars measured by real-time RT-PCR at different dark-time. The *FNR* transcript levels were normalized to that of *actin1* (internal control). (A) Changes in the *FNR* transcript levels of XS134 and Q4145 cultivars during the transition from light (0 min) to dark (1, 3 and 10 min), normalized to that of 0 min of each cultivar. (B) Comparison between the *FNR* expression levels of XS134 and Q4145 cultivars at different dark-time (1, 3 and 10 min). The relative expression level was normalized to that of Q4145. Error bars represent the standard deviation from three to four independent experiments.

so-called state 2 (low fluorescent state) goes to state 1 (high fluorescent state). In addition, Ceppi et al. (2012) suggested that the IP amplitude is correlated with changes in the PSI content of a leaf. Further, Schreiber et al. (1989) suggested that the IP phase corresponds to PSI fluorescence. However, our simulation data strongly support the theory of Duysens and Sweers (1963), in its modified version (Stirbet and Govindjee, 2011, 2012), suggesting that the IP phase is mainly related to the progressive photo-reduction of Q_A during the thermal J–I–P phase (Fig. 6A). Furthermore, the theory suggesting that a transient block in the electron acceptor side of PSI and, thus, a traffic jam of electrons on the electron transport chain is responsible for the IP rise phase (Munday and Govindjee, 1969; Schreiber and Vidaver, 1974; Satoh, 1981) and is in agreement with our simulation data. In fact, Figs. 5 and 6 show that the IP rise and the increase of the relative concentration of reduced PQ components occur under high [NADPH] conditions. This condition leads to a transient block on electron flow around PSI and a traffic jam of electrons formed in the electron transport chain, as a consequence of reduction of PSI acceptors during continuous illumination. Another argument in favor of the theory, mentioned above, has been proposed by Munday and Govindjee (1969), and extended by Schansker et al. (2005), suggesting that methyl viologen (MV) is able to bypass the transient block on the acceptor side of PSI leading to the disappearance of the IP phase. Based on our experimental and theoretical data, we suggest that the higher [NADPH]/[$NADP^+$] ratio might be a possible reason for the slightly higher IP rise observed in the elite cultivars, as a consequence of the transient block on electron transfer in the electron acceptor side of PSI (Fig. 1).

We have observed an increase in the minimum of I_{820} signal, which was accompanied by a significant delay in $P700^+$ reduction in the elite cultivars as compared to the landraces (Fig. 3). It is known that the I_{820} signal is mainly affected by the rate of electron flow from PSII to PSI (Schansker et al., 2003; Lazar, 2009). In other words, a decrease in the rate of electron donation from PSII to PSI is associated with decrease in the minimum of I_{820} signal. In fact, in the presence of DCMU (3,4-dichlorophenyl)-1,1-dimethylurea), which binds to the Q_B binding site on D1 protein of PSII causing a block on electron transfer from PSII to cyt b_6f, a strong decrease in the minimum of I_{820} signal has been observed, especially under long-time incubation with this inhibitor (Schansker et al., 2003). In addition, a similar effect was observed upon treatment with DBMIB (2,5-dibromo-3-methyl-6-isopropyl benzoquinone), which prevents oxidation of reduced PQ molecules by cyt b_6f, leading to a lack of ability to reduce oxidized PC and P700 (Schansker et al., 2005; Lazar, 2009). Contrary to the effect mentioned above, our experimental data showed an increase in the minimum of I_{820} signal in the elite cultivars, as compared to those in landraces. The logical

interpretation of this result should exclude a possible limitation on electron flow from PSII to PSI in the elite cultivars. However, a limitation on the acceptor side of PSI seems to be a plausible reason for it. It appears that the reversal of the transmission decrease of I_{820} signal in the time range between the I and P levels of Chl *a* fluorescence can be caused by a limitation on the acceptor side of PSI due to inactive FNR or to inactivity of the Calvin–Benson cycle (Carrillo et al., 1980; Satoh, 1981; Schreiber et al., 1988; Harbinson and Foyer, 1991; Foyer et al., 1992). Under these circumstances, all the redox components of the electron transport chain at the end of PSI become gradually reduced, with a long delay in their re-oxidation (Schansker et al., 2003). In addition, this transient blockage can promote a recombination reaction between FeS groups $(F_AF_B)^-$ and $P700^+$, which occurs with a halftime of about 43 ms (Jordan et al., 1998). Also, the cyclic electron transfer around PSI can contribute to the re-reduction of the oxidized P700 during the first 200–300 ms of fluorescence induction (Joliot and Joliot, 2002). Assuming that the elite cultivars initially have a higher [NADPH]/[$NADP^+$] ratio compared to the landraces, limitation on the acceptor side of PSI, caused by quick reduction of the electron transfer chain at the end of PSI, becomes more pronounced. The transient block on electron flow beyond P700 may cause less charge separation in PSI leading to an increase in the minimum of I_{820} signal. Such behavior has been observed when samples were excited with low light intensity (Lazar, 2009). Furthermore, significant correlation between the IP phase and $P700^+$ reduction rate, and their connection with F_v/F_m individually, suggests that these features are interdependent upon each other. Hence, the slight increase of F_v/F_m observed in elite cultivars compared to landraces may be related to high IP phase and low $P700^+$ reduction rate (Fig. 4 and Table 1). Yet, the mechanisms underlying these correlations remain unclear.

Variations in FNR: A possible mechanism underlying the observed variations of OJIP curves and I_{820} signal

Our working hypothesis is that the difference in the FNR activation/deactivation dynamics in darkness might be a possible mechanism underlying our observed differences between elite and landrace groups. Our idea was based on earlier work (Satoh and Katoh, 1980; Satoh, 1982; Carrillo and Vallejos, 1987; Schansker et al., 2006) which showed that FNR enzyme was related to the transient block on electron transfer on the acceptor side of PSI. It has been demonstrated earlier (Schansker et al., 2006) that the inactivation of FNR in darkness is plant species dependent. For example, it takes ~15 min in pea leaves for full inactivation, and it may take around 1 h in *Pinus halepensis* (Schansker et al., 2008). Therefore, the variations observed in the elite cultivars might originate from variations in the turnover rate of FNR enzyme during light/dark transitions, as compared to landraces. In other words, the FNR of the elite cultivars may take more time to be inactivated in darkness compared to those in landraces. During this time, the FNR enzyme can continue to reduce $NADP^+$ molecules, leading to initially high [NADPH]/[$NADP^+$] ratios during the OJIP induction. Under this circumstance, the NADP decreases in amount. Thus, the whole electron transport chain at the end of PSI becomes quickly reduced, causing less charge separation at P700, as shown in Fig. 3A. Then, this transient block on electron transfer on the acceptor side of PSI is probably shifted toward PSII, leading to an increase in the relative concentration of the reduced PQ located on the electron acceptor side of PSII (Fig. 6), parallel with an increase of IP phase (Figs. Fig. 1 and 5A). To confirm our hypothesis, simulation of Chl *a* fluorescence induction and I_{820} signal were performed under high [NADPH] and small NADP pool size conditions. Fig. 5B shows that the simulation data are in agreement with the experimental results, especially under high [NADPH]. It is important to note that this modeling analysis inherently assumes that during OJIP transient, certain levels of FNR activity is available, as suggested by Lazar (2009), and reaches its maximum after fluorescence has reached the P level (Schansker et al., 2003; Ilík et al., 2006). We assume that during OJIP transient, FNR does reduce $NADP^+$, which is available for electron transfer. A higher [NADPH]/[$NADP^+$] ratio will lead to a greater limitation on the acceptor side of PSI, and therefore a higher IP phase. However, beyond the P level, the Calvin–Benson cycle becomes gradually activated, thus consuming NADPH and generating $NADP^+$, which in turn removes the acceptor side limitation of PSI, and hence induces a gradual decay of the fluorescence level during the slow decreasing phase (PSMT). Therefore, lack of $NADP^+$ regeneration, during OJIP transient, may be a potential reason for a higher IP phase, rather than inactive FNR. However, more research is needed to quantify the dynamics of FNR activity during dark/light transitions.

Furthermore, we estimated the turnover rate of FNR in darkness by analyzing the correlation between the dark recovery of the IP phase and the *FNR* expression level in two representative cultivars XS134 and Q4145 (Figs. 7 and 8). Our result shows that the *FNR* expression level of XS134, which represents the elite group, remained unchanged during the first few minutes of light/dark transitions, leading to low IP phase recovery. Assuming that the activation state of FNR enzyme follows changes in the transcript level, our results suggest that this enzyme can lead to an increase of the [NADPH]/[$NADP^+$] ratio in darkness in the elite group. Besides the potential contribution of FNR to variations in [NADPH]/[$NADP^+$] ratio, we cannot exclude other possibilities that influence this ratio in a leaf. For example, rates of reactions related to NADPH generation, i.e., the pentose phosphate pathway, and NADPH consumption, i.e., the Calvin–Benson cycle, and amino acid synthesis under dark might differ between different rice accessions and hence influence the [NADPH]/[$NADP^+$] ratio in darkness.

Conclusions

In the present work, we have compared two photosynthetic parameters of two groups of Chinese rice, using simultaneous measurements of Chl *a* fluorescence induction and I_{820} transmission signal. We have shown that the elite cultivars exhibit a higher IP phase and a lower $P700^+$ accumulation compared to the landraces (Figs. Fig. 1, Fig. 3 and 5A). We suggest that such behavior originates from a transient block in electron transfer and a traffic jam on the electron acceptor side of PSI. An increase of [NADPH]/[$NADP^+$] ratio during light/dark transitions can be a possible mechanism generating these changes. The above proposal is in full agreement with our simulation data that shows an increase of the IP phase and a lowering of $P700^+$ accumulation under high [NADPH] conditions (Fig. 5B). A natural variation of the FNR activity during light/dark transitions is suggested to be a potential cause for the behavior observed in the elite cultivars (Figs. 7 and 8). Considering that the elite rice cultivars have undergone a strong artificial selection, we suggest a potential artificial selection of FNR during the breeding process.

One caveat we need to mention here is that, in this research, we have only used ten elite cultivars and ten landraces. Therefore, whether all current elite rice cultivars would show the changes observed in this work regarding the IP phase and the I_{820} signal is not yet known. However, the selection of elite and landraces does not influence the conclusion regarding the potential mechanism of simultaneous change of IP phase and I_{820} signal reported in this study. More work, using a larger sample size of elite and landrace accessions, is needed to test whether FNR might have been under artificial selection during the rice breeding process.

Acknowledgements

We thank the grant "Modeling and simulation of rice high yield and stable yields. Chinese Academy of Sciences (CAS) Strategic Research Project XDA08020301" for funding that allowed us to do this research. Govindjee thanks CAS for his visit to Shanghai

Appendix A. Supplementary data

Supplementary data associated with this article can be found, in the online version, at http://dx.doi.org/10.1016/j.jplph.2014.12.019.

References

Bao Y, Wei JQ, Zhao JM, Huang YL. Confirmed test about the condign density of transplantation on Kongyu-131. Reclaim Rice Cult 2006;S1:7–8.
Blankenship RE. Molecular mechanisms of photosynthesis. 2nd ed. Oxford, UK: Wiley-Blackwell; 2014.
Boisvert S, Joly D, Carpentier R. Quantitative analysis of the experimental O–J–I–P chlorophyll fluorescence induction kinetics apparent activation energy and origin of each kinetic step. FEBS J 2006;273:4770–7.
Bukhov NG, Sridharan G, Egorova EA, Carpentier R. Interaction of exogenous quinones with membranes of higher plant chloroplasts: modulation of quinone capacities as photochemical and non-photochemical quenchers of energy in Photosystem II during light–dark transitions. Biochim Biophys Acta 2003;1604:115–23.
Carrillo N, Lucero HA, Vallejos RH. Effect of light on chemical modification of chloroplast ferredoxin-NADP reductase. Plant Physiol 1980;65:495–8.
Carrillo N, Vallejos E. Ferredoxin-NADP+ oxidoreductase. In: Barber J, editor. The light reactions (topics in photosynthesis). Amsterdam: Elsevier; 1987. p. 527–60.
Ceppi MG, Oukarrouma A, Cicek N, Strasser RJ, Schansker G. The IP amplitude of the fluorescence rise OJIP is sensitive to changes in the photosystem I content of leaves: a study on plants exposed to magnesium and sulfate deficiencies, drought stress and salt stress. Physiol Plant 2012;144:277–88.
Deng HB, Deng QY, Chen LY, Yang YS, Liu GM, Zhuang W, et al. Yield-increasing effect of yield-enhancing QTLs from *O. rufipogon* transferred to 9311, a male parent of medium super hybrid rice. Hybrid Rice 2007;22:49–52.
Duysens LMN, Sweers HT. Mechanism of the two photochemical reactions in algae as studied by means of fluorescence. In: Studies on microalgae and photosynthetic bacteria Japanese. Tokyo: University of Tokyo Press; 1963. p. 353–72, Society of Plant Physiologists.
Photosynthesis: plastid biology, energy conversion and carbon assimilation. Eaton-Rye JJ, Tripathy BC, Sharkey TD, editors. Advances in photosynthesis and respiration including bioenergy and other processes, vol. 34. Dordrecht: Springer; 2012.
Evans JR. Improving photosynthesis. Plant Physiol 2013;162:1780–93.
Feng L, Wang K, Li Y, Tan Y, Kong J, Li H, et al. Overexpression of SBPase enhances photosynthesis against high temperature stress in transgenic rice plants. Plant Cell Rep 2007;26:1635–46.
Foyer CH, Lelandais M, Harbinson J. Control of the quantum efficiences of photosystem I and II, electron flow, and enzyme activation following dark-to-light transitions in pea leaves; relationship between NADP/NADPH ratios and NADP-malate dehydrogenase activation state. Plant Physiol 1992;99:979–86.
Photosystem I: the light-driven platocyanin: ferredoxin oxidoreductase. Golbeck JH, editor. Advances in photosynthesis and respiration including bioenergy and other processes, vol. 24. Dordrecht: Springer; 2006.
Govindjee, Björn LO. Dissecting oxygenic photosynthesis: the evolution of the Z-scheme for thylakoid reactions. In: Itoh S, Mohanty P, Guruprasad KN, editors. Photosynthesis: overviews on recent progress and future perspectives. New Delhi: IK Publishers; 2012. p. 1–27.
Govindjee. Sixty-three years since Kautsky: chlorophyll *a* fluorescence. Aust J Plant Physiol 1995;22:131–60.
Gowik U, Westhoff P. The path from C3 to C4 photosynthesis. Plant Physiol 2011;155:56–63.
Harbinson J, Foyer J. Relationship between the efficiencies of photosystem I and II and stromal redox state in CO_2-free air; evidence for cyclic electron flow *in vivo*. Plant Physiol 1991;97:41–9.
Harbinson J, Hedley CL. The kinetics of P-700$^+$ reduction in leaves: a novel in situ probe of thylakoid functioning. Plant Cell Environ 1989;12:357–69.
Harbinson J, Woodward FI. The use of light-induced absorbance changes at 820 nm to monitor the oxidation state of P-700 in leaves. Plant Cell Environ 1987;10:131–40.
Hsu BD, Leu KL. A possible origin of the middle phase of polyphasic chlorophyll fluorescent transient. Funct Plant Biol 2003;30:571–6.
Hunter CN, Daldal F, Thurnauer MC, Beatty JT. The purple photosynthetic bacteria. Advances in photosynthesis and respiration including bioenergy and other processes, vol. 28. Dordrecht: Springer; 2009.
Ilík P, Schansker G, Kotabová E, Váczi P, Strasser RJ, Barták M. A dip in the chlorophyll fluorescence induction at 0.2–2 s in Trebouxia-possessing lichens reflects a fast reoxidation of photosystem I. A comparison with higher plants. BBA 2006;1757:12–20.
Jiang GH, Xu CG, Tu JM, Li XH, He YQ, Zhang QF. Pyramiding of insect- and disease-resistance genes into an elite indica, cytoplasm male sterile restorer line of rice, 'Minghui 63'. Plant Breed 2004;123:112–6.
Joliot P, Joliot A. Cyclic electron transfer in plant leaf. Proc Natl Acad Sci USA 2002;99:10209–14.
Jordan R, Nessau U, Schlodder E. Charge recombination between reduced iron-sulfur clusters and P700$^+$. In: Garab G, editor. Photosynthesis: mechanisms and effects. Dordrecht: Kluwer; 1998. p. 663–6.
Kalaji HM, Schansker G, et al. Frequently asked questions about in vivo chlorophyll fluorescence: practical issues. Photosynth Res 2014., http://dx.doi.org/10.1007/s11120-014-0024-6.
Ke B. Photosynthesis: photobiochemistry and photobiophysics. Advances in photosynthesis and respiration including bioenergy and other processes, vol. 10. Dordrecht: Springer; 2001.
Klughammer C, Schreiber U. An improved method, using saturating light pulses, for the determination of photosystem I quantum yield via P700$^+$-absorbance changes at 830 nm. Planta 1994;192:261–8.
Lazar D. Chlorophyll *a* fluorescence induction. Biochim Biophys Acta 1999;1412:1–28.
Lazar D. Modelling of light-induced chlorophyll *a* fluorescence rise (O–J–I–P transient) and changes in 820 nm-transmittance signal of photosynthesis. Photosynthetica 2009;47:483–98.
Leegood RC. C4 photosynthesis: principles of CO_2 concentration and prospects for its introduction into C3 plants. J Exp Bot 2002;53:581–90.
Livak K, Schmittgen TD. Analysis of relative gene expression data using real-time quantitative PCR and the 2-ΔΔCT method. Methods 2001;25:402–8.
Long SP, Zhu XG, Naidu SL, Ort DR. Can improvement in photosynthesis increase crop yields? Plant Cell Environ 2006;29:315–30.
Munday JC, Govindjee. Light-induced changes in the fluorescence yield of chlorophyll *a* in vivo; III. The dip and the peak in the fluorescence transient of *Chlorella pyrenoidosa*. Biophys J 1969;9:1–21.
Murchie EH, Pinto M, Horton P. Agriculture and the new challenges for photosynthesis research. New Phytol 2008;181:532–52.
Ort DR, Zhu XG, Melis A. Optimizing antenna size to maximize photosynthetic efficiency. Plant Physiol 2011;155:79–85.
Oukarroum A, Goltsev V, Strasser RJ. Temperature effects on pea plants probed by simultaneous measurements of the kinetics of prompt fluorescence, delayed fluorescence and modulated 820 nm reflection. PLoS ONE 2013;8:e59433, http://dx.doi.org/10.1371/journal.pone.0059433.
Chlorophyll *a* fluorescence: a signature of photosynthesis. Papagergiou GC, Govindjee, editors. Advances in photosynthesis and respiration including bioenergy and other processes, vol. 29. Dordrecht: Springer; 2004.
Parry MAJ, Andralojc PJ, Scales JC, Salvucci ME, Carmo-Silva AE, Alonso H, et al. Rubisco activity and regulation as targets for crop improvement. J Exp Bot 2013;64:717–30.
Pospisil P, Dau H. Chlorophyll fluorescence transients of photosystem II membrane particles as a tool for studying photosynthetic oxygen evolution. Photosynth Res 2000;65:41–52.
Prasil O, Kolber Z, Berry JA, Falkowski PG. Cyclic electron flow around photosystem II in vivo. Photosynth Res 1996;48:395–410.
Raines CA. Increasing photosynthetic carbon assimilation in C3 plants to improve crop yield: current and future strategies. Plant Physiol 2011;155:36–42.
Reynolds MP, Ginkel MV, Ribaut JM. Avenues for genetic modification of radiation use efficiency in wheat. J Exp Bot 2000;51:459–73.
Samson G, Bruce D. Origins of the low yield of chlorophyll *a* fluorescence induced by single turnover flash in spinach thylakoids. Biochim Biophys Acta 1996;1276:147–53.
Samson G, Prasil O, Yaacoub B. Photochemical and thermal phases of chlorophyll *a* fluorescence. Photosynthetica 1999;37:163–82.
Satoh K, Katoh S. Light-induced changes in chlorophyll *a* fluorescence and cytochrome f in intact spinach chloroplasts: the site of light-dependent regulation of electron transport. Plant Cell Physiol 1980;21:907–16.
Satoh K. Fluorescence induction and activity of ferredoxin-NADP$^+$ reductase in *Bryopsis* chloroplasts. Biochim Biophys Acta 1981;638:327–33.
Satoh K. Mechanism of photoactivation of electron transport in intact Bryopsis chloroplasts. Plant Physiol 1982;70:1413–6.
Schansker G, Srivastava A, Govindjee Strasser J. Characterisation of the 820-nm transmission signal paralleling the chlorophyll *a* fluorescence rise (OJIP) in pea leaves. Funct Plant Biol 2003;30:785–96.
Schansker G, Toth SZ, Strasser RJ. Dark recovery of the Chl *a* fluorescence transient (OJIP) after light adaptation: the q*T*-component of non-photochemical quenching is related to an activated photosystem I acceptor side. Biochim Biophys Acta 2006;1757:787–97.
Schansker G, Toth SZ, Strasser RJ. Methylviologen and dibromothymoquinone treatments of pea leaves reveal the role of photosystem I in the Chl *a* fluorescence rise OJIP. Biochim Biophys Acta 2005;1706:250–61.
Schansker G, Yuan Y, Strasser RJ. Chl a fluorescence and 820 nm transmission changes occurring during a dark-to-light transition in pine needles and pea leaves: a comparison. In: Allen JF, Osmond B, Golbeck JH, Gantt E, editors. Energy from the Sun. Dordrecht: Springer; 2008. p. 945–9.
Schreiber U, Klughammer C, Neubauer C. Measuring P700 absorbance changes around 830 nm with a new type of pulse modulation system. Z Naturforsch 1988;43c:686–98.

Schreiber U, Neubauer C, Klughammer C. Devices and methods for room-temperature fluorescence analysis. Philos Trans R Soc London 1989;323:241–51.

Schreiber U, Vidaver W. Chlorophyll fluorescence induction in anaerobic *Scenedesmus obliquus*. Biochim Biophys Acta 1974;368:97–112.

Schreiber U, Vidaver W. The I-D fluorescence transient; an indicator of rapid energy distribution changes in photosynthesis. Biochim Biophys Acta 1976;440:205–14.

Shevela D, Björn LO, Govindjee. Oxygenic photosynthesis. In: Razeghifard R, Hoboken NJ, editors. Natural and artificial photosynthesis: solar power as an energy source. Oxford, UK: John Wiley and Sons; 2013. p. 13–64.

Stirbet A, Govindjee. Chlorophyll *a* fluorescence induction: Understanding the thermal phase, the J-I-P rise. Photosynth Res 2011;113:15–61.

Stirbet A, Govindjee. On the relation between the Kautsky effect (chlorophyll *a* fluorescence induction) and photosystem II: basics and applications of the OJIP fluorescence transient. J Photochem Photobiol B: Biol 2012;104:236–57.

Strasser RJ, Michael MT, Qiang S, Goltsev V. Simultaneous in vivo recording of prompt and delayed fluorescence and 820-nm reflection changes during drying and after rehydration of the resurrection plant *Haberlea rhodopensis*. Biochim Biophys Acta 2010;1797:1313–26.

Vernotte C, Etienne AL, Briantais JM. Quenching of the system II chlorophyll fluorescence by the plastoquinone pool. Biochim Biophys Acta 1979;545:519–27.

Wydrzynski T, Satoh K, Photosystem II. The light-driven water: plastoquinone oxidoreductase. Advances in photosynthesis and respiration including bioenergy and other processes, vol. 22. Dordrecht: Springer; 2005.

Xin CP, Yang J, Zhu XG. A model of chlorophyll *a* fluorescence induction kinetics with explicit description of structural constraints of individual photosystem II units. Photosynth Res 2013., http://dx.doi.org/10.1007/s11120-013-9894-2.

Zhang X, Wang J, Huang J, Lan H, Wang C, Yin C, et al. Rare allele of OsPPKL1 associated with grain length causes extra-large grain and a significant yield increase in rice. Proc Natl Acad Sci USA 2012;109:21534–9.

Zhou J, Yao Q. Agronomic features and high-yield cultivation techniques for Xiushui-134. China Rice 2012;18:78–9.

Zhu XG, Govindjee Baker NR, Sturler ED, Ort DR, Long SP. Chlorophyll *a* fluorescence induction kinetics in leaves predicted from a model describing each discrete step of excitation energy and electron transfer associated with photosystem II. Planta 2005;223:114–33.

Zhu XG, Long SP, Ort DR. Improving photosynthetic efficiency for greater yield. Ann Rev Plant Biol 2010;61:235–61.

Zhu XG, Long SP, Ort DR. What is the maximum efficiency with which photosynthesis can convert solar energy into biomass? Curr Opin Biotechnol 2008;19:153–9.